



**Fermi National Accelerator Laboratory**

TM-1542

**Studies of Time Dependence of Fields in  
TEVATRON Superconducting Dipole Magnets\***

R. W. Hanft, B. C. Brown, D. A. Herrup,  
M. J. Lamm, A. D. McInturff, and M. J. Syphers  
Fermi National Accelerator Laboratory  
P.O. Box 500, Batavia, Illinois

August 22, 1988

\*Presented at the 1988 Applied Superconductivity Conference, San Francisco, California, August 21-25, 1988.



# STUDIES OF TIME DEPENDENCE OF FIELDS IN TEVATRON SUPERCONDUCTING DIPOLE MAGNETS

R. W. Hanft, B. C. Brown, D. A. Herrup,  
M. J. Lamm, A. D. McInturff, M. J. Syphers

Fermi National Accelerator Laboratory<sup>+</sup>  
P. O. Box 500  
Batavia, Illinois 60510

## Abstract

The time variation in the magnetic field of a model Tevatron dipole magnet at constant excitation current has been studied. Variations in symmetry allowed harmonic components over long time ranges show a log t behavior indicative of "flux creep". Both short time range and long time range behavior depend in a detailed way on the excitation history. Similar effects are seen in the remnant fields present in full-scale Tevatron dipoles following current ramping. Both magnitudes and time dependences are observed to depend on details of the ramps, such as ramp rate, flattop duration, and number of ramps. In a few magnets variations are also seen in symmetry unallowed harmonics.

## Introduction

Operation of the Tevatron in colliding beams mode has focused attention on the time behavior of magnetic fields in Tevatron magnets during periods when the excitation current is sensibly constant. Tevatron studies have found chromaticities changing with time during injection;<sup>1</sup> this has been linked to changing sextupole fields in the Tevatron dipole magnets. In this paper we report studies of time variations of harmonic field components in such magnets.

## Description of Magnet

The superconducting Tevatron dipole magnet has a magnetic length of 6.116 m and a radial mechanical aperture of 0.0381 m (1.5 inches). The coil package is assembled from an upper coil and a lower coil each of which has an inner layer of 35 turns and an outer layer of 21 turns. The Rutherford style cable is composed of 23 strands, 12 coated with ebanol and 11 with Stabrite. Each strand has 2050 NbTi filaments ~9 microns in diameter, the filament separation to diameter ratio is 0.35 and the copper to superconductor ratio is 1.8 by volume. The coil package is enclosed in a cylindrical cryostat inserted into a warm iron yoke. The transfer function of this magnet is 9.96 gauss/ampere, where 18.6% of the dipole field comes from the iron. One TeV operation corresponds to an excitation current of 4.5 kA. The critical currents I<sub>c</sub> at 5.0 T, 4.2 K, 2 x 10<sup>-12</sup> Ω-cm vary from 5000 to 5820 A for most of the cable, but toward the end of the production run values of 6250 A were obtained.

## Definition of Field Harmonics

using the harmonic expansion

$$B^* = B_0 \sum_n c_n^* (z/\rho)^n \quad (1)$$

where  $B^* = B_x - iB_y$  are the magnetic field components,

<sup>+</sup>Work supported by the U. S. Department of Energy

$z = x + iy$ ,  $B_0$  is the dipole field (in the y-direction), and  $\rho$  is a normalization length conventionally set to two-thirds of the mechanical aperture, in this case 0.0254 m (1 inch). The coefficients  $c_n^* = a_n + ib_n$ , where  $a_n$  are known as the skew coefficients and  $b_n$  the normal coefficients, respectively. For a perfectly constructed magnet having both up-down and left-right symmetry, only  $b_n$ ,  $n$  even, can be non-zero, i.e., are "symmetry allowed"; and these  $b_n$  can be adjusted in the design. Non-zero  $b_n$ ,  $n$  odd, require left-right asymmetry. Non-zero  $a_n$ ,  $n$  odd, require up-down asymmetry; and non-zero  $a_n$ ,  $n$  even, require both left-right and up-down asymmetries. Up-down asymmetries can result from mechanical size differences between the upper and lower coils or from different critical current  $J_c(B_0)$  properties of these coils. The  $a_n$  and  $b_n$  as defined here are dimensionless but have values dependent on the choice of  $\rho$ . These  $a_n$  and  $b_n$  are usually reported in terms of "units", which means a factor of 10<sup>-4</sup> is suppressed. The overall phase angle is determined such that  $\alpha_0 = 0$  and  $b_0 = 1.0$ . For remnant fields, no  $B_0$  factor is extracted and no factor of 10<sup>-4</sup> suppressed; field strengths  $A_n$  and  $B_n$  at radius  $\rho$  are reported in gauss.

The Tevatron dipole has significant higher order harmonics designed into the coil shape:  $b_6 = +5.35$  units,  $b_8 = -12.46$  units, and  $b_{10} = +3.70$  units. The ends are "naturally" wound which results in large negative  $b_2$  there. To compensate, the body field is designed to have  $b_2 = +13.4$  units due to transport current in the windings. The body field values of  $b_2$  (and  $b_4$ ) can be varied without materially changing the other allowed harmonics by adjusting the so-called key shims; magnets having body field  $b_2$  near zero also have been built.

## Previously Observed Hysteretic Behavior

When a newly cooled magnet is ramped for the first time, the observed value of  $b_2$  falls rapidly to an algebraic minimum at ~25 A and then rises toward the transport current value at higher excitation currents. On the down-ramp the value of  $b_2$  rises above the transport value and continues to rise as the current falls to 0 A. On the next up-ramp  $b_2$  falls rapidly to an algebraic minimum at ~175 A, where it is considerably more positive than it was on the first ramp; the second ramp value then rises and joins the trace from the previous up-ramp. Similar hysteretic behavior has been seen in all allowed  $b_n$ . In the normal decapole  $b_4$  the up-ramp values are algebraically more positive than the down-ramp values, that is, the reverse of the situation with  $b_2$ . This hysteretic behavior is understood in terms of the fields due to so-called persistent currents which are induced within the NbTi filaments to oppose penetration of magnetic field; these persistent current related fields add to the transport current fields. Static models are qualitatively successful in describing this behavior and showing its functional dependence on parameters such as filament diameter.<sup>2,3</sup>

The harmonic data for the Tevatron magnets<sup>4</sup> was obtained as follows: The magnets were ramped several

Manuscript received August 22, 1988.

times up to 4000 A and back down to 0 A. Then the excitation current was raised to the first desired current and held constant while the harmonics were measured. Then the current was further raised to a new target current, which was again held constant during another harmonics measurement. Neither the ramp rate nor any time delay in taking data at constant current was thought to be important; the data presented herein show this is not quite true.

### Experiment Details

#### Production Measurements Facility

Since the completion of the production run the Fermilab MTF facility for testing full-scale Tevatron magnets has been operated episodically for the testing of small numbers of rebuilt and newly constructed magnets. The harmonic measuring system in this facility has been described previously<sup>5</sup>; it has been used unchanged to study time dependent effects in some Tevatron dipoles tested during these episodic runs. Because of unsatisfactory long-term current stability from the power supplies, investigations with this system have concentrated on remnant field behavior at 0 A. Significant features of the harmonics measuring system are recounted here. The 2.39 m long probe was positioned longitudinally in the center of the magnet. The magnet was ramped to 1000 A, and a standard measurement made. The direction of the dipole field was determined for use in subsequent decomposition of amplitudes into normal and skew components. The voltage signal from the rotating sense coil was Fourier analyzed to extract the various harmonic amplitudes. It is thought that there is essentially no true 16-pole ( $a_7$  and  $b_7$ ) in these magnets; any 16-pole obtained in the Fourier analysis is then interpreted as a feed-down effect from the strong designed-in normal 18-pole ( $b_8$ ) due to the probe's axis of rotation being displaced from the magnet axis. Elimination of the 16-pole allows determination of the displacement values  $\Delta x$  and  $\Delta y$ , which in turn allows eliminating feed-down effects in all other harmonics as well. The magnet was then quenched to still any persistent currents and to return the magnet to the "standard state". Measurements made after quenching show a remnant dipole field of 7.0 to 7.3 gauss and a remnant normal sextupole of  $\sim -0.2$  gauss; all other harmonics were virtually zero. These remnant fields are thought to be due to the iron yoke. Dipole TB0447 was followed for a 14 hour period after a quench; no change in remnant fields was observed. Following the post-quench measurement the magnet was ramped in a specified way; and after the excitation current returned to 0 A, a succession of remnant measurements made. Since the probe requires 10 seconds for one rotation and system overhead restricts consecutive runs to at least 60 seconds separation, short time structure features can not be studied. On the other hand measurements can easily be extended over many hour periods. All reported remnant data use the dipole direction and the probe displacement corrections determined by the pre-quench 1000 A run, and the iron remnants are subtracted. The coil temperature was 4.6 K.

#### R & D Facility

A second test facility primarily for R & D work exists, where "model" Tevatron magnets are studied in vertical Dewars. These models are 0.81 m long; the iron yoke is absent. A Morgan coil rotating at 6 Hz provides signal to a BNL-style magnetometer<sup>6</sup>. Voltage signals from a single rotation are processed during the subsequent rotation thus providing a maximum data rate of about 3 Hz. Measurements are sometimes made "on the fly", i.e., while the magnet excitation current is

changing; and in addition to the usual voltage signal arising from the probe rotation there is also a small contribution from the change in impressed field. The 0.47 m long probe was positioned to sample only body field. There is no 16-pole probe winding, and no correction is made due to the decentering of the probe rotation axis relative to the coil axis. All data runs began with quenching the magnet. Most data were taken at 4.2 K. Studies show that the power system can hold currents steady to within 0.1 A for long periods, and transitions from current ramps to constant current can be made with less than 0.2 A over or undershoot.

### Experimental Data

#### Model Magnet

Thus far only the model designated RL1001 has been intensively studied. The cable critical current  $I_c$  (4.2 K, 5 T) of this magnet is about +0.3 units. Following a quench, the magnet was ramped at 100 A/s to 400 A, and that current held for 1800 s. In a companion run, after a quench, the magnet was ramped at 100 A/s to 4000 A and then down to 400 A, and the 400 A held for 1800 s. In both runs there was no parabolic roll-on to the constant current "porch". At 400 A  $B_0 = 3245$  gauss,  $b_2$  on an up-ramp (down-ramp) = -22.0 (+18.2) units, respectively. The time evolutions of  $b_2$  are shown in figure 1, where the sign of  $b_2$  from the first run data has been reversed to facilitate visual comparison. The zero of the time axis is at the beginning of the porch. When the porch follows an up-ramp,  $b_2$  becomes more positive on the porch; when the porch follows a down-ramp,  $b_2$  becomes more negative. For  $t > 10$  s the up ramp data are linear in  $\log t$ , which is indicative of "flux creep"<sup>7</sup>. The slope of the first run is +0.30 units/time decade = 0.097 gauss/time decade. Note how the data in the second run initially decrease rapidly, and then near  $t = 100$  s begin to decrease more slowly at a rate similar to the first run.

Normal Sextupole on 400 A Porch

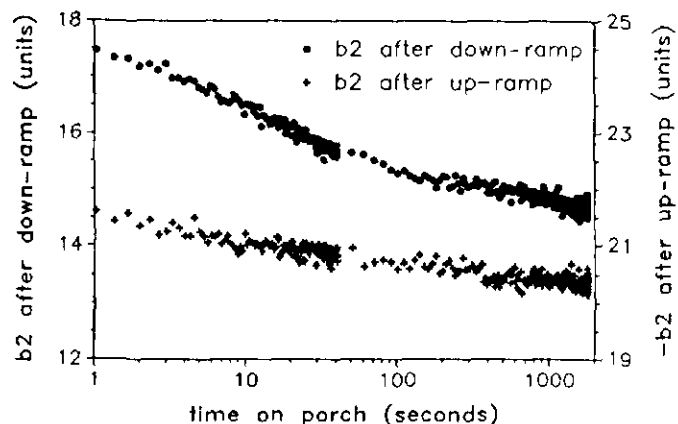


Figure 1. Time evolution of the normal sextupole on a 400 A porch. The magnet was ramped at 100 A/s from 0 A to the 400 A porch (up-ramp data) and from 0 A to 4000 A to the 400 A porch (down-ramp data). Note that the up-ramp data are plotted with the sign of  $b_2$  reversed.

In another group of runs this magnet was ramped at 25 A/s, 100 A/s, and 200 A/s to 800 A and held at that current for 30 minutes. Behavior at 800 A is particularly interesting to us because the dipole field produced is nearly the same as it is in the Tevatron at injection. Figure 2 shows  $b_2$  at 800 A plotted against a linear time scale for the first 40 seconds to show more

clearly the short time behavior. The three runs are each represented by the lines shown. For the 100 A/s data the individual data points are also shown, and their scatter reflects the measuring system resolution. The point  $b_2 = -7.6$  units at  $t = 0$  s is obtained by interpolating data taken in companion runs on ramps at 25 A/s that continue above 800 A. The rate of rise during the first 10 s clearly depends on the ramp rate prior to the porch. Thereafter in each run  $b_2$  continues to increase linearly with  $\log t$ . To the precision of our measurements the slopes in all three runs are 0.24 units/time decade = 0.16 gauss/time decade. For  $t > 40$  s the 200 A/s  $b_2$  data are 0.35 units more positive than the 25 A/s data.

### Normal Sextupole on 800 A Porch

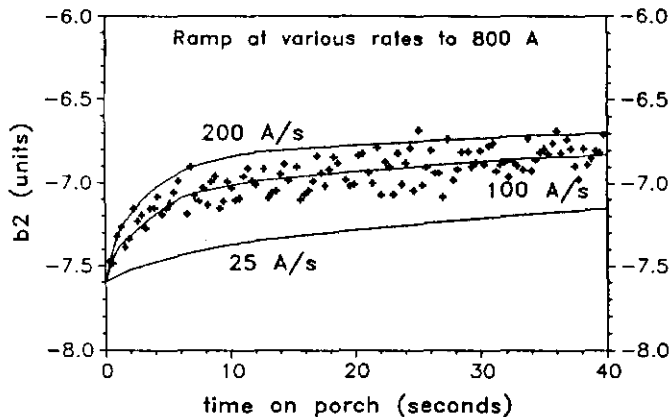


Figure 2. Time evolution of the sextupole on an 800 A porch on an up-ramp. The magnet was ramped at 25 A/s (line only), 100 A/s (data points and line), and 200 A/s (line only) from 0 A to the 800 A porch.

The sextupole data obtained on a porch at 800 A on the first down-ramp are shown in figure 3. These data also show a ramp rate dependence, but the changes during the first several seconds are more pronounced than on the corresponding up-ramps.

### Normal Sextupole on 800 A Porch

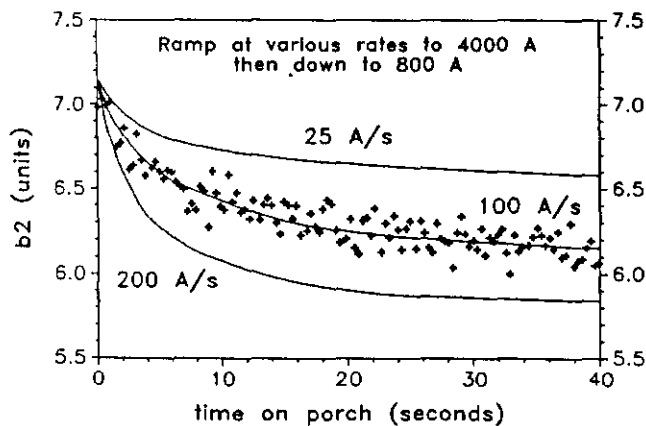


Figure 3. Time evolution of the sextupole on an 800 A porch on a down-ramp. The magnet was ramped from 0 A to 4000 A and then down to the 800 A porch at 25 A/s (line only), 100 A/s (data points and line), and 200 A/s (line only).

The actual situation in the Tevatron during colliding beam operation has been simulated. A fixed target mode ramp cycle was executed six times: Ramp up to a 30 s 4878 A flattop at 110 A/s and then down to 490 A. The dwell at 490 A between cycles was 2 s. After the sixth cycle the current was ramped up to an

injection porch at 812 A and held at that current for some time. Then the up-ramp was resumed. Appropriate parabolic roll-on to and roll-off of the porch were included in the current waveform. The behaviors of  $b_2$  and  $b_4$  during a porch of 6 hours duration are shown in figure 4, where the sign of  $b_4$  has been reversed to aid visual comparison. These  $b_2$  data show an approximate  $\log t$  behavior, but there is some structure particularly at large  $t$ . The average rate of change of  $b_2$  is 0.50 units/time decade, which is considerably faster than observed when the 800 A porch was reached on the first up-ramp after a quench. In addition to this run at 4.2 K, runs were made at 3.6 K and 3.2 K. At lower temperatures  $b_2$  at the start of the porch has more negative values as expected in simple theories due to the increase of  $J_c$  with decreasing temperature. The observed value of  $\Delta b_2^5$ /time decade is the same at all three temperatures. Previous work with superconducting cylinders has shown that logarithmic creep is only weakly temperature dependent<sup>8</sup>.

### b2 & b4 on Injection Porch

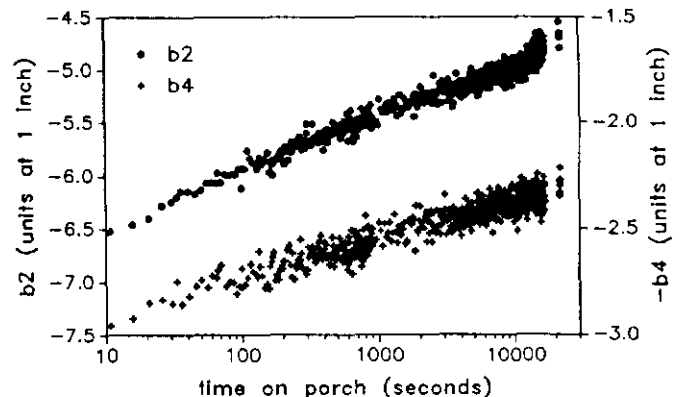


Figure 4. Time evolution of sextupole and decapole on the injection porch at 812 A of an accelerator-like current waveform. Note that the  $b_4$  data are plotted with sign reversed.

The change in  $b_2$  as the ramp was resumed after a porch of 1800 s duration is shown in figure 5.

### Sextupole on Accelerator Ramp

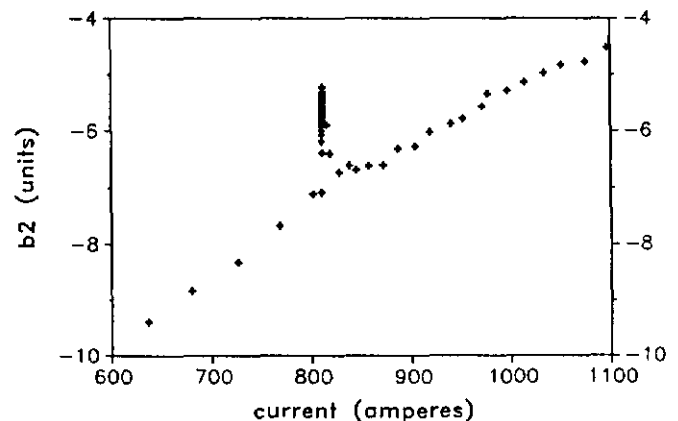


Figure 5. Sextupole as a function of current during an accelerator-like current waveform. The up-ramp stops at 812 A for 1800 s, during which the sextupole becomes more positive; and then the up-ramp resumes.

It is observed that  $b_2$  drops rapidly back to the value it had at the start of the porch, i.e., to the value it had on continuous up-ramps that have no porch. We

have varied the time structure in the current waveform roll-off and conclude that during that time  $b_2$  is a function of the excitation current  $I$  and not  $dI/dt$ .  
Production Line Magnets

Remnant fields were studied in seven dipoles passing through the production test facility; six were randomly chosen and the seventh, TB0223, was deliberately selected because all 23 strands in its cable are ebanol coated.

Figure 6 shows the time decay of the remnant sextupole in these seven magnets after each had been quenched and ramped once at 110 A/s to a 1 s long flattop at 4000 A. The point where the ramp cycle returns to 0 A is taken as the 0 of the time axis. After the return to 0 A these magnets show remnant dipoles (iron contribution subtracted) of 6.0 to 8.1 gauss, normal sextupoles  $B_2$  at radius  $\rho$  of 6.0 to 8.1 gauss, normal decapoles  $B_4$  - 0.5 to - 0.8 gauss, and normal 14-poles  $B_6$  +0.56 to 0.8 gauss. All other harmonics, except as noted below, are virtually zero. In this and subsequent figures care is needed in interpreting the first point plotted at 14 seconds elapsed time, where the time scale for changes in harmonics may be less than the probe rotation time. For four magnets the sextupole decay shows an initial rapid decay which then turns to log  $t$  behavior after a few hundred seconds. This is not inconsistent with the time structure seen in the model magnet's data taken on the 400 A and 800 A porches on the down-ramp of the first ramp cycle as reported above. A fifth magnet TB0271 shows slightly different behavior. For these magnets, the larger the initial remnant sextupole at the end of the ramp cycle, the slower the subsequent decay. The magnitude of the initial sextupole is proportional to the maximum quench currents obtained for these magnets. The all ebanol magnet TB0223 and especially TB0447 show different behaviors. In all seven magnets the decay of the remnant dipole follows the decay of the sextupole indicating that both fields arise from the same currents. With the possible exception of TB0447,  $B_4$  decay follows  $B_2$  decay.

### Remnant Sextupoles

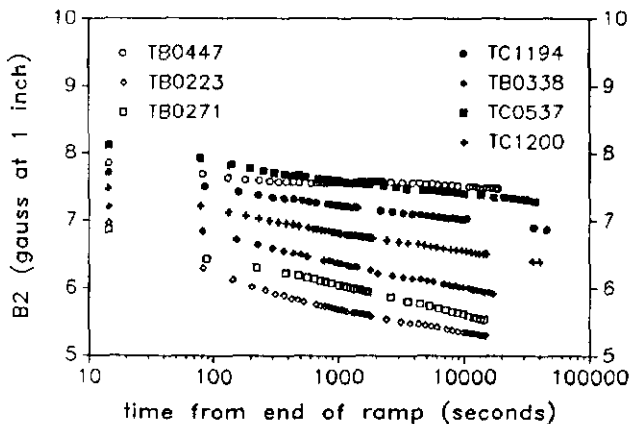


Figure 6. Decay of the remnant sextupole after a single ramp cycle at 110 A/s to a 1 s 4000 A flattop.

Figure 7 shows the skew quadrupole fields  $A_1$  after the magnets were ramped as above. In this figure TC1200 is representative of the four magnets showing similar remnant sextupole behavior; these magnets show little skew quadrupole signal. In TB0447 and TB0223 the value of  $A_1$  changes with time. We interpret this as indicating that the time development of the currents is different in the upper coil relative to the lower coil due to the detailed properties of the cable in each coil. Such a situation would likely maintain left-right

symmetry, and so no time dependence in the normal quadrupole would be expected, and none is seen. A developing up-down asymmetry that produces a changing  $A_1$  would likely produce a changing skew octupole  $A_3$  as well, and we so observe.

### Remnant Skew Quadrupoles

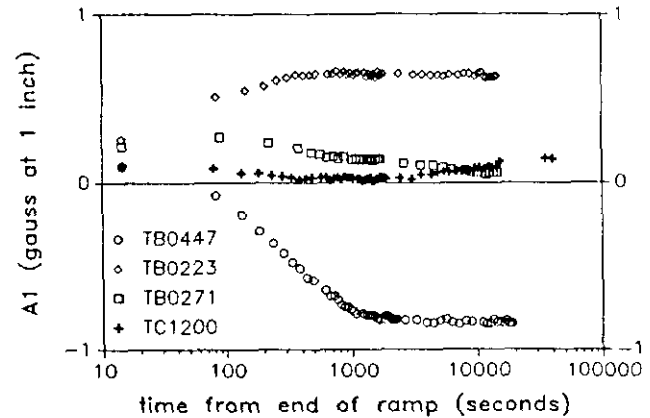


Figure 7. Time evolution of remnant skew quadrupoles after a single ramp cycle at 110 A/s to a 1 s 4000 A flattop.

We studied the effect of making multiple consecutive ramps. Data from TC1194 are shown in Figure 8. As the number of ramps is increased, the remnant sextupole observed at the end of the final ramp decreases in magnitude; and the remnant sextupole decays more quickly, i.e., the slope of the data is larger when starting with smaller sextupoles. These differences in the remnant behavior are most pronounced between data taken after one ramp and two ramps. The trend in creep rates is similar to that seen in the 800 A porch data.

### Effect of Number of Ramps

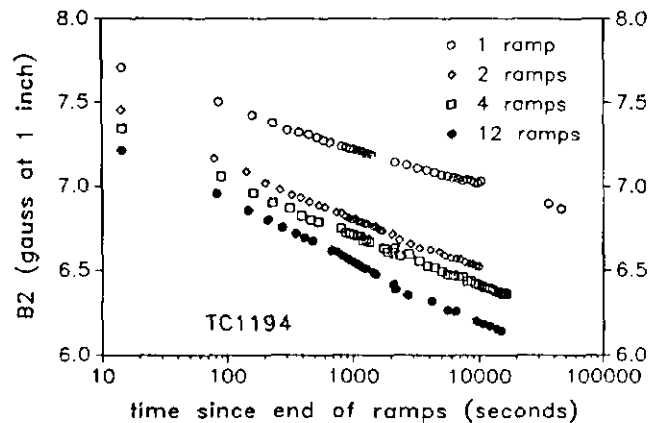


Figure 8. The effect on remnant sextupole behavior caused by making multiple consecutive ramps prior to measurement.

The effect of changing the flattop duration during a single ramp at 110 A/s to 4000 A and back to 0 A is shown in Figure 9. Longer duration flattops result in lower initial sextupoles, and the subsequent decay deviates from being linear in log  $t$ .

## Effect of Duration of Flattop

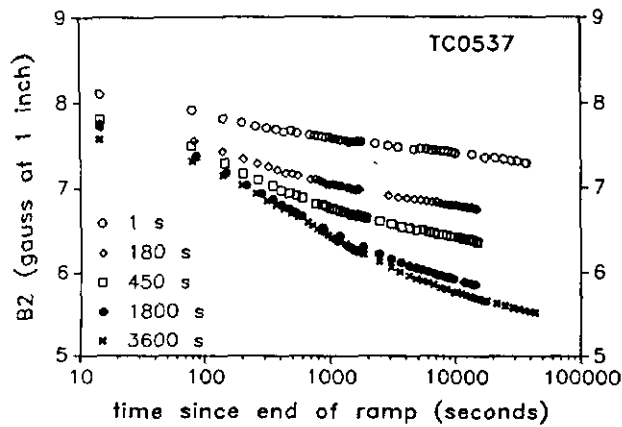


Figure 9. The effect on remnant sextupole behavior caused by varying the duration of the 4000 A flattop on a single ramp at 110 A/s.

The ramp rate in a ramp cycle to a 1 s 4000 A flattop was varied; the data are shown in figure 10. Slower ramp rates yield larger remnant sextupoles which initially decay more slowly. At longer times the decay rate of the slow ramp data exceeds that of the high ramp data.

## Effect of Ramp Rate

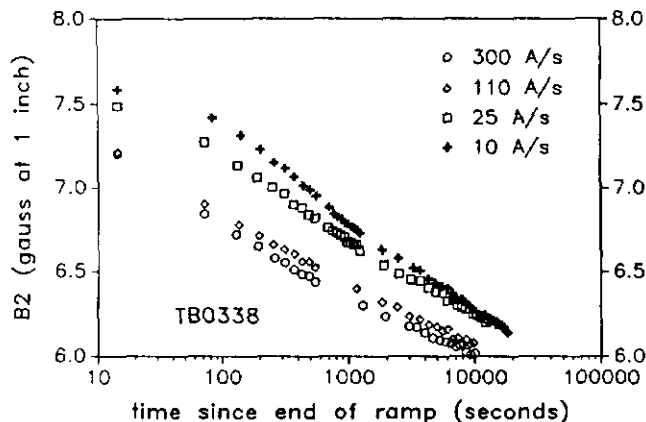


Figure 10. The effect in remnant sextupole behavior caused by varying the ramp rate in a single ramp cycle to a 1 s 4000 A flattop.

## Conclusion

In this paper we present considerable data. In many situations the time evolution of field harmonics exhibits a log  $t$  dependence indicative of "flux creep". Detailed understanding is not yet available, and it is clear that a complete description must accommodate other processes.<sup>9</sup>

## References

[1] D. A. Finley, D. A. Edwards, R. W. Hanft, R. Johnson, A. D. McInturff, and J. Strait, "Time Dependent Chromaticity Changes In the Tevatron," Proceedings of the 1987 IEEE Particle Accelerator Conference, Washington, D.C., p. 151, March 16-19, 1987. Also Fermilab publication FN-451, March 1987.

[2] M. A. Green, "Residual Fields in Superconducting Magnets," IEEE Trans. on Nucl. Sci. NS-18, No. 3, pp. 664-664 (1971); M. A. Green, "Residual Fields in Superconducting Magnets," Proc. of the Magnet Technology Conference MT-4, p. 339, 1972.

[3] B. C. Brown, H. E. Fisk, and R. Hanft, "Persistent Current Fields in Fermilab Tevatron Magnets," IEEE Trans. on Magnetics, 21, No. 2, pp. 979-982, March 1985.

[4] R. Hanft, B. C. Brown, W. E. Cooper, D. A. Gross, L. Michelotti, E. E. Schmidt, and F. Turkot, "Magnetic Field Properties of Fermilab Energy Saver Dipoles," IEEE Trans. Nuc. Sci. NS-32, pp. 3381-3384, August 1983; R. Hanft, "Lengthwise Variation in Field Harmonics of Tevatron Dipoles", Proceedings of the 1984 Summer Study on the Design and Utilization of the Superconducting Super Collider, pp. 432-344, 1984.

[5] B. C. Brown, W. E. Cooper, J. D. Garvey, D. A. Gross, R. Hanft, K. P. Kaczar, J. E. Pachnik, C. W. Schmidt, E. E. Schmidt, and F. Turkot, "Report on the Production Magnet Measuring System for the Fermilab Energy Saver Superconducting Dipoles and Quadrupoles," IEEE Proc. on Nuc. Sci. NS-30, No. 4, pp. 3608-3610, August 1983.

[6] G. H. Morgan, "Stationary Coil for Measuring the Harmonics in Pulsed Transport Magnets," Proc. Inter. Conf. on Magnet Technol., edited by Y. Winterbottom, p. 787, 1972.

[7] P. W. Anderson, "Theory of Flux Creep in Hard Superconductors," Phys. Rev. Lett., pp. 309-311, 1962.

[8] M. R. Beasley, R. Labusch, and W. W. Webb, "Flux Creep in Type-II Superconductors," Phys. Rev., 181, pp. 682-700, 1969.

[9] D. A. Herrup, M. J. Syphers, D. E. Johnson, R. P. Johnson, A. V. Toilestrup, R. W. Hanft, B. C. Brown, M. J. Lamm, M. Kuchnir, A. D. McInturff, "Time Variations of Fields in Superconducting Magnets and Their Effects on Accelerators," paper LH-3 presented at this conference.